Toward Emotion Recognition in Car-Racing Drivers: A Biosignal Processing Approach

Christos D. Katsis, Nikolaos Katertsidis, George Ganiatsas, and Dimitrios I. Fotiadis, *Senior Member, IEEE*

***Abstract*—In this paper, we present a methodology and a wearable system for the evaluation of the emotional states of car-racing drivers. The proposed approach performs an assessment of the emotional states using facial electromyograms, electrocardiogram, respiration, and electrodermal activity. The system consists of the following: 1) the multisensorial wearable module; 2) the centralized computing module; and 3) the system's interface. The system has been preliminary validated by using data obtained from ten subjects in simulated racing conditions. The emotional classes identified are high stress, low stress, disappointment, and euphoria. Support vector machines (SVMs) and adaptive neuro-fuzzy inference system (ANFIS) have been used for the classification. The overall classification rates achieved by using tenfold cross validation are 79.3% and 76.7% for the SVM and the ANFIS, respectively.**

***Index Terms*—Adaptive neuro-fuzzy inference system (ANFIS), biosignal processing, emotion recognition, support vector machines (SVMs), wearable system.**

I. Introduction

AS IT IS commonly conceived, emotion is bound up with feeling. If we want to produce an off-the-cuff definition of the term, we would probably make some reference to subjective feelings. Emotion is a bodily state involving various physical structures; it is gross or fine-grained behavior, and it occurs in particular situations. When we use the term, we mean any or all of these possibilities, each of which may show a wide range of variations. This indicates the major difficulty which besets the study of the subject. Any theory of emotion or any empirical research on emotion involves only some part of the broad meaning of the term. After over a century of research, emotion theorists still do debate upon what emotions are and how they are communicated. Emotion comprises more than its outward physical expression; it also consists of internal feelings and thoughts, as well as other internal processes of which the person having the emotion may not be aware [1]. Traditionally, the fields of psychology and psychophysiology have sought features which indicate common emotional states across large populations, despite the fact that there exist wide variations in individual response patterns due to gender, personality, and ethnic background [2].

Emotions often involve both thinking and feeling; both are cognitively experienced events and physical changes in the body. Although there is no technology that can truly read our thoughts, there exist a growing number of sensors which can capture various physical manifestations of emotion: video recordings of facial expressions and posture or gesture changes [3], vocal inflection changes [4], skin-surface sensing of muscle tension, electrocardiogram (ECG), electrodermal activity (EDA), blood-glucose levels, and other bodily changes [5], [6]. Most work in automatic understanding of affective condition has focused on the classification of the universal expressions defined by Ekman and Friesen [7]. Thus, the implemented algorithms were tailored toward developing models to recognize the universal expressions from static images or video sequences [3], [4], [8]–[12]. There are also methods employing a combination of audio and video signals for emotion recognition [5], [13]–[15]. One of the hallmarks in emotion theory is whether distinct physiological patterns accompany each emotion [6]. Ekman *et al.* [16] and Winton *et al.* [17] provided some of the first findings showing significant differences in autonomic nervous system signals according to a small number of emotional categories, but there was no exploration of automated classification. Flidlund and Izard [18] appear to be the first who applied pattern recognition (linear discriminants) on the classification of four different emotions (happiness, sadness, anger, and fear) from physiological signals, attaining rates of 38%–51% accuracy. Similar efforts aimed at finding physiological correlates, focusing on t-tests or analysis of variance comparisons [19], [20]. The latest findings indicate that emotional state is reflected in human biosignals; thus, emotion recognition methodologies based on the classification of extracted series of features from these biosignals are constantly gaining popularity [21]–[24].

The inability to manage one's emotions while driving is identified as one of the major causes of accidents [25]. When drivers are overwhelmed by anger or stress, their thinking, perceptions, and judgments are impaired, leading to misinterpretation of events. In addition, drivers often lack the ability to calm themselves when they are angry or frustrated. In the

Manuscript received November 22, 2006; revised March 14, 2007. This work was supported in part by the European Commission (EC) under AUBADE Project IST-2002-507605 and in part by the Greek Secretariat for Research and Technology under PENED Project 03ED139. This paper was recommended by Associate Editor Y. Xiao.

C. D. Katsis is with the Department of Medical Physics, Medical School and the Unit of Medical Technology and Intelligent Information Systems, Department of Computer Science, University of Ioannina, 45110 Ioannina, Greece.

N. Katertsidis and G. Ganiatsas are with the Unit of Medical Technology and Intelligent Information Systems, Department of Computer Science, University of Ioannina, 45110 Ioannina, Greece.

D. I. Fotiadis is with the Unit of Medical Technology and Intelligent Information Systems, Department of Computer Science, University of Ioannina, 45110 Ioannina, Greece, and also with the Biomedical Research Institute—Foundation for Research and Technology Hellas, 45110 Ioannina, Greece (e-mail: fotiadis@cs.uoi.gr).

Color versions of one or more of the figures in this paper are available online at http://ieeexplore.ieee.org.

Digital Object Identifier 10.1109/TSMCA.2008.918624

context of car racing, similar situations are not even tolerable since they may not only compromise the performance of the drivers but also endanger their lives. Generally speaking, the optimum way to recognize emotions is by employing a variety of methods (primarily speech and image–video processing) in order to exploit and combine the advantages of each method. In our case (car-racing drivers), recognizing and classifying emotions using advanced image and video processing algorithms are not feasible (due to the use of safety casque), and speech-based methods provide poor results due to the noisy environment inside the car.

In this paper, we introduce an automated approach in emotion recognition, which is based on several biosignals. Our methodology has been integrated into a wearable system which is able to estimate the emotional state of car-racing drivers by classifying features extracted from facial electromyograms (EMGs), ECG, respiration, and EDA. Our system consists of the following: 1) the multisensorial wearable which is responsible for the acquisition, preprocessing, and wireless transmission of the selected biosignals; 2) the centralized module which extracts special features from the aforementioned biosignals and estimates the subject's emotional state (high stress, low stress, disappointment, and euphoria) based on a dataset containing the extracted features along with the medical experts' annotation; and 3) the system user interface.

In the following sections, first, we provide information on the selected biosignals and present our methodology, and then, we describe the system's modules and their functionalities. The evaluation of the system using recordings acquired during simulated car-race driving conditions is given next. Finally, the limitations and applications of the proposed approach are presented in Section IV.

II. Materials and Methods

A. Selected Biosignals

Emotions involve physiological responses which are regulated by the brain. Through our nervous system, we perceive the world, adapt our stress, coordinate all body parts and functions, express our emotions, and create our conscious reality. When we are frightened, our heart races, our breathing becomes rapid, our mouth becomes dry, our muscles tense, and our palms may become sweaty. These bodily changes are mediated by the autonomic nervous system, which controls heart muscle, smooth muscle, and exocrine glands and operates with the somatic motor system, to regulate most types of behavior, whether in normal or emergency situations [26]. Certain emotions may result in a wide variety of bodily reactions, which can be monitored and measured. Our objective is to use these reactions and, by means of special biosensors, to deduce the emotional state of the user. An important aspect in this process is the selection of signals which constitute the input to the emotion recognition system. We have considered the following set of biosignals.

EMG: It refers to the muscle activity or the frequency of muscle tension of a certain muscle. Research using surface EMG has extended observations, documenting patterns of skeletomotor activity which differentiate both within and between emotional and cognitive processes [18], [19], [27]. In addition, muscle activity has been shown to increase during stress. People may unconsciously clench their muscles in a state of mental stress or fatigue even when no physical activity is required [28]. Firing from a muscle could indicate either unconscious clenching due to stress or firing due to motion.

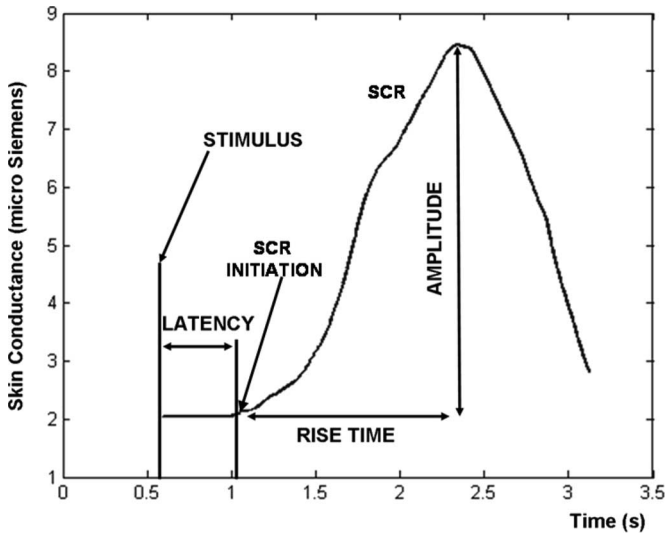

Fig. 1. Graphical representation of the SCR.

ECG: The ECG signal is the manifestation of contractile activity of the heart, which is a valuable indicator of the individual's overall activity level. For example, heart-rate accelerations occur in response to exercise, emotional states, loud noise, sexual arousal, and mental effort [29]. Furthermore, lower heart rate is generally associated with a relaxed state or a state of experiencing pleasant stimuli.

Respiration: Respiration is an indicator of how deep and fast a person is breathing. Emotional excitement and physical activity lead to faster and deeper respiration, whereas peaceful rest and relaxation lead to slower and shallower respiration [30]. A state of stress would therefore be indicated by frequent respiration; however, sudden stressors, such as startle, tend to cause momentary cession of respiration.

EDA: It is also referred as skin conductance activity because of the underlying principle of measurement. EDA describes alterations—in skin's ability to conduct electricity—occurring due to interactions between environmental events and an individual's psychophysiological state. More specifically, it is related to the sympathetic nervous system activity, and it has been associated with measures of emotion, arousal, and attention [21]. The EDA reading is typically characterized by two components: a tonic baseline level and short-term phasic responses superimposed on it. Phasic responses (momentary increases in skin conductance) determine the event-related responses occurring in an individual, due to environmental stimuli. The characteristics of a typical skin conductance response (SCR) resemble a peak and are shown in Fig. 1. EDA is one of the most robust and well-studied physiological measures. It has been previously employed in assessing the difficulty of driving tasks [31], in determining stress in anticipatory anxiety studies [32], and as part of lie detectors [33].

TABLE I
FEATURES EXTRACTED FOR EACH OF THE ACQUIRED BIOSIGNALS (FACIAL EMG, ECG, RESPIRATION, AND EDA)

EMG	ECG	respiration	EDA
Mean Value	Mean amp	Mean amp	Mean amp of Skin Conductance Responses
Root Mean Square	Heart Rate	Respiration Rate	Rate of Skin Conductance Responses
	Mean_abs_first_difference	Mean_abs_first_difference	Mean_abs_first_difference
			Mean rise duration of Skin Conductance Response

B. Biosignal Processing

Body movement may affect readings from sensors. In order to compensate for any artefacts generated, a preprocessing stage is employed, consisting of low-pass filters at 100 and 500 Hz for the ECG and the facial EMG, respectively, and smoothing (moving average) filters for the respiration and EDA signals. The preprocessed signals are then passed on to the feature-extraction module. The set of features selected in this paper provides a combination of simple statistics and complicated characteristics which are physically motivated and aimed at capturing the underlying nature of the physiological signals. They are also intended to compensate for day-to-day variations and differences between individuals. The extracted features from each signal are shown in Table I and are described next.

Mean Value: It is the mean value for a 10-s window of each signal.

Root Mean Square (RMS): For a signal $X_N = (x_1, x_2, \ldots, x_N)$, it is defined as

$$\text{RMS} = \sqrt{\frac{1}{N}\sum_{i=1}^{N} x_i^2} = \sqrt{\frac{x_1^2 + x_2^2 + \cdots + x_N^2}{N}} \quad (1)$$

where N is the number of samples contained in the 10-s window.

Mean_abs_fd: For a signal $X_N = (x_1, x_2, \ldots, x_N)$, the mean absolute first difference (mean_abs_fd) is defined as

$$\text{mean\_abs\_fd} = \sum_{1}^{N} \frac{|x_2 - x_1| + |x_3 - x_2| + \cdots + |x_N - x_{N-1}|}{N} \quad (2)$$

where N is the number of samples contained in the 10-s window. This feature is an approximation of the first derivative and, therefore, corresponds to fast changes in the recorded biosignals.

Mean amp: For the ECG signal, the maximum amplitude for every ECG beat that occurs in a period of 10 s is calculated; then, the mean amplitude is defined as the average value of the computed amplitudes. For the respiration signal, it is the mean value of the chest cavity expansions occurred in a time window of 10 s. For the EDA signal, it is the mean value of the increases in skin conductance between SCR initiations and SCR peaks (see Fig. 1), which occurred in a 10-s time window.

Mean rise dur: It is the mean value of the temporal intervals between SCR initiations and SCR peaks, which occurred in a 10-s time window.

Rate: It is the heart rate, respiration rate, and number of SCRs per minute, which are calculated every 10 s.

C. Classification

Several theorists have proposed sets of basic emotions. These sets either span the space of emotion or provide a palette from which all other emotions can be derived. As an example, the basic emotion set proposed by Ekman [34] includes anger, fear, disgust, sadness, and enjoyment and, sometimes, surprise. One of the difficulties of using emotion classes is that the relationship between the emotion categories is not clear. There is no structure for measuring the similarity of the emotions or the way in which they differ. This makes the boundaries of what is included in each category difficult to define. For example, the specifications for separating distress from fear or contempt and disgust are subject to debate. In recognition experiments, frameworks which allow differences between emotions to be measured along some metric of similarity provide greater flexibility in designing experiments and offer greater insight into misclassification errors. Frameworks that support similarity metrics include the arousal–valence space used by Lang *et al.* [35] and the circumplex model proposed by Russell [36]. The arousal–valence space is the one adopted in our approach and defines the emotion space using an arousal axis ranging from calm to excited and a valence axis ranging from negative to positive. In this space, four emotional classes are chosen by the psychologists involved in the experiment (high stress, low stress, disappointment, and euphoria).

The classification into the predefined emotional classes is achieved by using the following classifiers.

Support Vector Machine (SVM): A classification task based on SVM involves training and testing which consist of a number of data instances. Each instance in the training set contains one "target value" (class label) and several "attributes." The goal of the SVM is to produce a model which predicts a target value of data instances in the testing set in which only the attributes are given. Let a training set of instance-label pairs

be (x_i, y_i), $i = 1, \ldots, l$, where $x_i \in \Re^n$ is the training vector belonging to one of the four emotional classes, l is the number of the extracted features in the training set, and y_i indicates the class of x_i. The SVM requires the solution of the following optimization problem:

$$\min_{w,b,\xi} \left(\frac{1}{2}\mathbf{w}^{\mathrm{T}}\mathbf{w} + C\sum_{i=1}^{l} \xi_i \right) \tag{3}$$

subject to

$$y_i \left(\mathbf{w}^{\mathrm{T}} \varphi(x_i) + b \right) \geq 1 - \xi_i, \qquad \xi_i \geq 0 \tag{4}$$

where b is the bias term, $\mathbf{w}$ is a vector perpendicular to the hyperplane $\langle \mathbf{w}, b \rangle$, ξ is the factor of classification error, and $C > 0$ is the penalty parameter of the error term [37]. The training vectors x_i are mapped into a higher dimensional space F by the function $\phi : R^n \rightarrow F$. The SVM finds a separating hyperplane with the maximal geometric margin and the minimal empirical risk R_{emp} in the higher dimensional space. R_{emp} is defined as

$$R_{\mathrm{emp}}(a) = \frac{1}{2l}\sum_{i=1}^{l} |y_i - f(x_i, a)| \tag{5}$$

where f is the decision function defined as

$$f(x) = \sum_{i=1}^{l} y_i a_i K(x_i, x) + b \tag{6}$$

where $K(x_i, x_j) \equiv \varphi(x_i)^{\mathrm{T}} \varphi(x_j)$ is the kernel function, and a_i is the weighting factor. In our case, we have selected the radial basis function (RBF) kernel

$$K(x_i, x_j) = \exp\left(-\gamma \|x_i - x_j\|^2\right), \qquad \gamma > 0 \tag{7}$$

where $\gamma = 1/2\sigma^2$ (σ is the standard deviation) is a kernel parameter. The RBF kernel nonlinearly maps samples into a higher dimensional space; thus, it can handle the case when the relation between class labels and attributes is nonlinear. The parameters γ and C were defined heuristically after a series of experiments, and more specifically, γ was set equal to $2^{2.3}$, and C was set equal to 2^7. In our application, we have used the SVM algorithm of the LIBSVM library [38].

Adaptive Neuro-Fuzzy Inference System (ANFIS): Neuro-fuzzy techniques have emerged from the fusion of artificial neural networks and fuzzy inference systems and form a popular framework for solving real world problems. A neuro-fuzzy system is based on a fuzzy system which is trained by a learning algorithm derived from neural network theory. ANFIS [39] is an architecture which is practically an evolution of a Sugeno-type fuzzy system [40]. To present the ANFIS architecture, two fuzzy if–then rules based on a first-order Sugeno model are considered

$$\text{Rule 1: If } (x \text{ is } A_1) \text{ and } (y \text{ is } B_1), \text{ then } (f_1 = p_{1x} + q_{1y} + r_1) \tag{8}$$

$$\text{Rule 2: If } (x \text{ is } A_2) \text{ and } (y \text{ is } B_2), \text{ then } (f_2 = p_{2x} + q_{2y} + r_2) \tag{9}$$

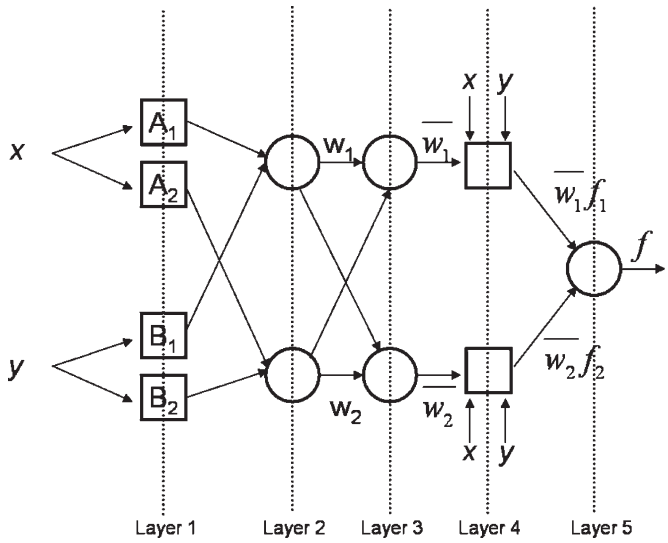

Fig. 2. ANFIS architecture. Adaptive layers (layers 1 and 4) are shown in squares.

where x and y are the inputs, A_i and B_i are the fuzzy sets, f_i are the outputs within the fuzzy region specified by the fuzzy rule, and p_i, q_i, and r_i are the design parameters which are determined during the training process. The ANFIS architecture which implements these two rules is shown in Fig. 2. In the first layer, all the nodes are adaptive nodes. The outputs of layer 1 are the fuzzy membership grade of the inputs, which are given as

$$O_i^1 = \mu_{A_i}(x), \qquad i = 1, 2 \tag{10}$$

$$O_i^1 = \mu_{B_{i-2}}(y), \qquad i = 3, 4 \tag{11}$$

where $\mu_{A_i}(x)$ and $\mu_{B_{i-2}}(y)$ can adopt any fuzzy membership function. For example, if the bell-shaped membership function is employed, $\mu_{A_i}(x)$ is given as

$$\mu_{A_i}(x) = \frac{1}{1 + \left| \frac{x - c_i}{a_i} \right|^{2b_i}} \tag{12}$$

where $\{a_i, b_i, c_i\}$ is the parameter set referred to as premise parameters.

In the second layer, the nodes are fixed nodes. The outputs of this layer can be represented as

$$O_i^2 = w_i = \mu_{A_i}(x)\mu_{B_i}(y), \qquad i = 1, 2 \tag{13}$$

which are also called the firing strengths of the rules.

In the third layer, the firing strengths are normalized. The outputs of this layer can be represented as

$$O_i^3 = \overline{w_i} = \frac{w_i}{w_1 + w_2}, \qquad i = 1, 2. \tag{14}$$

In the fourth layer, the nodes are adaptive. The output of each node in this layer is the product of the normalized firing strength and a first-order polynomial (for a first-order Sugeno model). Thus, the outputs of this layer are given as

$$O_i^4 = \overline{w_i} f_i = \overline{w_i}(p_i x + q_i y + r_i), \qquad i = 1, 2. \tag{15}$$

In the fifth layer, there is only one single fixed node. This node performs the aggregation of all incoming signals. Hence, the overall output of the model is

$$O_i^5 = \sum_{i=1}^{2} \overline{w_i} f_i = \frac{\sum_{i=1}^{2} w_i f_i}{w_1 + w_2}, \qquad i = 1, 2. \tag{16}$$

The task of the learning algorithm for this architecture is to tune all the modifiable parameters, namely, $\{a_i, b_i, c_i\}$ and $\{p_i, q_i, r_i\}$, to make the ANFIS output match the training data. When the premise parameters a_i, b_i, and c_i of the membership function are fixed, the output of the ANFIS model can be written as

$$f = \frac{w_1}{w_1 + w_2} f_1 + \frac{w_2}{w_1 + w_2} f_2. \tag{17}$$

Substituting (14) into (17) yields

$$f = \overline{w_1} f_1 + \overline{w_2} f_2. \tag{18}$$

Substituting the fuzzy if–then rules into (18), we obtain

$$f = \overline{w_1}(p_1 x + q_1 y + r_1) + \overline{w_2}(p_2 x + q_2 y + r_2) \tag{19}$$

which can be expressed as

$$f = (\overline{w_1} x p_1 + (\overline{w_1} y) q_1 + (\overline{w_1}) r_1 + (\overline{w_2} x) p_2 + (\overline{w_2} y) q_2 + (\overline{w_2}) r_2 \tag{20}$$

which is a linear combination of the modifiable parameters p_1, q_1, r_1, p_2, q_2, and r_2. Least squares method can be used to identify the optimal values of these parameters easily. A hybrid algorithm combining the least squares method and the gradient descent method is adopted for training in our case. This algorithm is composed of a forward pass and a backward pass. The least squares method (forward pass) is used to optimize the consequent parameters with the premise parameters fixed. Once the optimal consequent parameters are found, the backward pass starts immediately. The gradient descent method (backward pass) is used to optimally adjust the premise parameters corresponding to the fuzzy sets in the input domain. The output of the ANFIS is calculated by employing the consequent parameters found in the forward pass. The output error is used to adapt the premise parameters by means of a standard backpropagation algorithm. It has been proven that this hybrid algorithm—utilized in our approach—is highly efficient in training the ANFIS [39].

D. System Architecture

To use the proposed methodology, which is described next, we have developed a wearable system which consists of the following: 1) the multisensorial wearable; 2) the centralized module; and 3) the system's interface. The architecture of our system is shown in Fig. 3. A more detailed description of the system's modules and their functionalities follows.

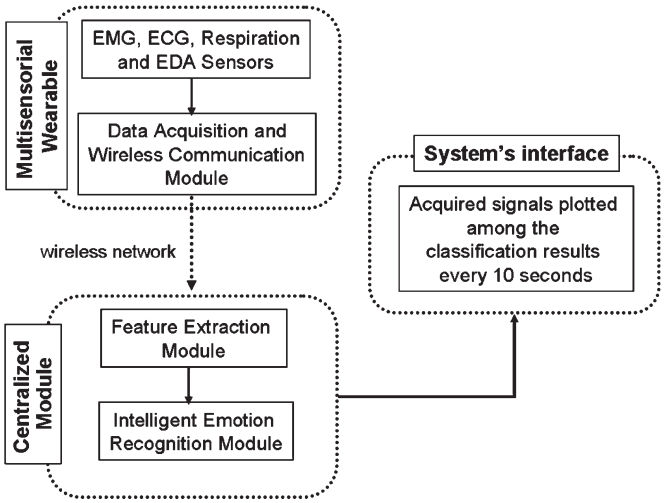

Fig. 3. Proposed system architecture.

Multisensorial Wearable: It is a noninvasive, ergonomic, comfortable, and easy to use wearable which includes a number of state-of-the-art sophisticated biosensors gathering raw physiological data (facial EMG, ECG, respiration, and EDA). The wearable is composed of four pieces: 1) the balaclava containing the EMG textile fireproof sensors; 2) the ECG and respiration sensors on the thorax of the driver; 3) the EDA textile and fireproof sensor placed inside the driver's glove; and 4) the data acquisition and wireless communication module. The data acquisition module collects, filters, and preprocesses all the biosignals obtained from the sensors of the wearable. It is small in size, highly integrated, and scalable in order to fit into the car. The collected raw signals are recorded in the data acquisition unit, rectified, and filtered before being sent wirelessly to the centralized system for further processing and decision making. Finally, the communication module is activated by the system end user and is responsible for the secure transfer of the biosignals collected and processed by the data acquisition unit. The user measurements are transferred through a wireless connection (IEEE 802.11b) to the centralized module for further analysis. The multisensorial wearable is shown in Fig. 4.

Centralized Module: It is the core module of the system. It is divided into two major modules, namely, the feature-extraction module and the intelligent emotion recognition module. The first extracts features from the selected biosignals to be used by the intelligent emotion recognition module in order to determine a subject's emotional state. The intelligent emotion recognition module performs a near real-time classification of the subject's emotional state based on predefined emotional classes (high stress, low stress, disappointment, and euphoria). The subject's emotional state is being monitored during the driving task, whereas the classification results, which are the final outcome of this module, are updated every 10 s.

System's Interface: The end users of the system are able to view, and save the acquired biosignals obtained from the sensors located on the driver as well as the emotional state of the subject, through the system's interface.

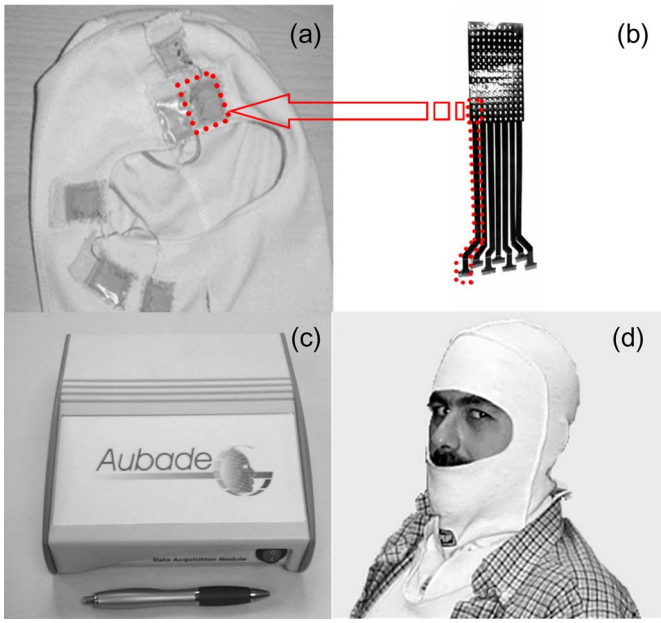

Fig. 4. Multisensorial wearable. (a) Wearable balaclava containing the EMG sensors. (b) EMG thin flexible grid sensors. The material used as electrode carrier (Polyimid, 50 μm thick) allows grids to be cut out in any required shape or size according to the size of the recorded muscle. (c) Data acquisition module. (d) Subject wearing the multisensorial mask.

III. Results

The following measures were used in order to evaluate the performance of our system: 1) sensitivity (Sen_x),[1] given in (21) and shown at the bottom of the page; 2) positive predictive accuracy (PPA_x)[2] or positive predictive, given in (22) and shown at the bottom of the page. We also measured the Accuracy (Acc) which is defined as the ratio of the number of correctly classified events to the total number of events

$$\text{Acc} = \frac{\#\text{ of correctly classified emotional events}}{\text{total }\#\text{ of emotional events}} \times 100\%. \tag{23}$$

In order to minimize the bias associated with the random sampling of the training and testing data samples in comparing the predictive accuracy of two or more methods, we use k-fold cross validation. In the k-fold cross validation, the complete dataset is randomly split into k mutually exclusive subsets of approximately equal size. The classification model is trained and tested k times. Each time, it is trained on all but one fold and tested on the remaining single fold. The cross-validation estimate of the overall accuracy is calculated as simply the average of the k individual accuracy measures

$$\text{CVA} = \sum_{i=1}^{k} C_i \tag{24}$$

where CVA stands for cross-validation accuracy, k is the number of folds used, and C_i is the corresponding accuracy measure of each fold. Since the CVA depends on the random assignment of the individual cases into k distinct folds, a common practice is to stratify the folds themselves. In the stratified k-fold cross validation, the folds are created in a way that they contain approximately the same proportion of predictor labels as the original dataset. Studies showed that the stratified cross validation tends to generate results with lower bias and lower variance when compared with the regular k-fold cross validation [41]. In this paper, to estimate the performance of the classifiers, a stratified tenfold cross-validation approach is used. Empirical studies showed that ten seems to be an optimal number of folds that optimizes the time it takes to complete the test while minimizing the bias and variance associated with the validation process [42].

The biosignals are obtained from car drivers in a controlled environment which uses a virtual reality room to provide realistic driver's conditions. This is implemented in a 3-D projection system, and the driver is equipped with visualization glasses which provide a realistic environment capturing the central notion and features of real racing; it also creates resembling stimuli and responses. Data come from ten healthy males which have average or high level driving skills. Drivers are selected and classified in the corresponding categories after an interview process, in which facts like years of driving experience and type of driving license were assessed as well. Four persons, aged 22–35, have above average driving skills, and six persons, aged 29–34, have professional driving skills. Each driver participated in eight driving rounds with average duration from 3 to 4 min. Drivers are not required to provide self-annotations of their emotional state during driving since this would compromise the realism of the conducted experiment.

[1]Sensitivity demonstrates the probability of correct identification of a specific emotion provided that the subject experiences this emotion.

[2]PPA demonstrates the probability of correct identification provided a positive finding of the specific emotion.

$$\text{Sen}_x = \frac{\#\text{ of emotional events correctly classified into group } x \text{ according to the system}}{\text{total }\#\text{ of emotional events belonging to group } x \text{ according to psychologists}} \times 100\% \tag{21}$$

$$\text{PPA}_x = \frac{\#\text{ of emotional events correctly classified into group } x \text{ according to the system}}{\text{total }\#\text{ of emotional events classified into group } x \text{ according to system}} \times 100\% \tag{22}$$

TABLE II
RESULTS OF THE STRATIFIED TENFOLD CROSS VALIDATION ACHIEVED WHEN SVM IS USED

Fold #	Classifier: SVM					
1	$Sen_{hi\ stress}$	0.806	$PPA_{hi\ stress}$	0.763	Acc	0.796
	$Sen_{low\ stress}$	0.758	$PPA_{low\ stress}$	0.806		
	$Sen_{disappointment}$	0.828	$PPA_{disappointment}$	0.632		
	$Sen_{euphoria}$	0.797	$PPA_{euphoria}$	0.917		
2	$Sen_{hi\ stress}$	0.657	$PPA_{hi\ stress}$	0.821	Acc	0.789
	$Sen_{low\ stress}$	0.909	$PPA_{low\ stress}$	0.698		
	$Sen_{disappointment}$	0.759	$PPA_{disappointment}$	0.667		
	$Sen_{euphoria}$	0.812	$PPA_{euphoria}$	0.903		
3	$Sen_{hi\ stress}$	0.600	$PPA_{hi\ stress}$	0.875	Acc	0.775
	$Sen_{low\ stress}$	0.909	$PPA_{low\ stress}$	0.667		
	$Sen_{disappointment}$	0.733	$PPA_{disappointment}$	0.647		
	$Sen_{euphoria}$	0.817	$PPA_{euphoria}$	0.879		
4	$Sen_{hi\ stress}$	0.778	$PPA_{hi\ stress}$	0.757	Acc	0.778
	$Sen_{low\ stress}$	0.758	$PPA_{low\ stress}$	0.714		
	$Sen_{disappointment}$	0.759	$PPA_{disappointment}$	0.629		
	$Sen_{euphoria}$	0.797	$PPA_{euphoria}$	0.917		
5	$Sen_{hi\ stress}$	0.806	$PPA_{hi\ stress}$	0.935	Acc	0.833
	$Sen_{low\ stress}$	0.818	$PPA_{low\ stress}$	0.794		
	$Sen_{disappointment}$	0.862	$PPA_{disappointment}$	0.676		
	$Sen_{euphoria}$	0.843	$PPA_{euphoria}$	0.894		
6	$Sen_{hi\ stress}$	0.694	$PPA_{hi\ stress}$	0.862	Acc	0.774
	$Sen_{low\ stress}$	0.909	$PPA_{low\ stress}$	0.769		
	$Sen_{disappointment}$	0.724	$PPA_{disappointment}$	0.600		
	$Sen_{euphoria}$	0.771	$PPA_{euphoria}$	0.831		
7	$Sen_{hi\ stress}$	0.722	$PPA_{hi\ stress}$	0.839	Acc	0.784
	$Sen_{low\ stress}$	0.879	$PPA_{low\ stress}$	0.784		
	$Sen_{disappointment}$	0.793	$PPA_{disappointment}$	0.561		
	$Sen_{euphoria}$	0.768	$PPA_{euphoria}$	0.914		
8	$Sen_{hi\ stress}$	0.833	$PPA_{hi\ stress}$	0.833	Acc	0.827
	$Sen_{low\ stress}$	0.879	$PPA_{low\ stress}$	0.829		
	$Sen_{disappointment}$	0.759	$PPA_{disappointment}$	0.759		
	$Sen_{euphoria}$	0.829	$PPA_{euphoria}$	0.853		
9	$Sen_{hi\ stress}$	0.806	$PPA_{hi\ stress}$	0.806	Acc	0.774
	$Sen_{low\ stress}$	0.758	$PPA_{low\ stress}$	0.735		
	$Sen_{disappointment}$	0.690	$PPA_{disappointment}$	0.526		
	$Sen_{euphoria}$	0.800	$PPA_{euphoria}$	0.933		
10	$Sen_{hi\ stress}$	0.778	$PPA_{hi\ stress}$	0.800	Acc	0.799
	$Sen_{low\ stress}$	0.788	$PPA_{low\ stress}$	0.765		
	$Sen_{disappointment}$	0.690	$PPA_{disappointment}$	0.667		
	$Sen_{euphoria}$	0.859	$PPA_{euphoria}$	0.871		

The following set of sensors is used:

1) four EMG thin flexible sensors which are placed on the left and right frontalis and the left and right masseter muscles (sampling rate: 1 kHz);
2) a three-lead ECG sensor which is attached to the thorax (sampling rate: 500 Hz);
3) a Hall-effect respiration sensor which is placed on the diaphragm (sampling rate: 50 Hz);
4) an EDA sensor which is attached to the index and middle fingers on the palm side of the left hand (sampling rate: 50 Hz).

Three cameras are used to record each driver round. The first captures the driver's face, the second captures the driver's round event, and the third captures a general view of the whole scene. Three experienced psychologists annotated the person's emotional state every 10 s. Annotation conflicts were resolved

TABLE III
RESULTS OF THE STRATIFIED TENFOLD CROSS VALIDATION ACHIEVED WHEN ANFIS IS USED

Fold #	Classifier: ANFIS					
1	Sens_hi stress	0.778	PPA_hi stress	0.778	Acc	0.766
	Sens_low stress	0.727	PPA_low stress	0.750		
	Sens_disappointment	0.793	PPA_disappointment	0.575		
	Sens_euphoria	0.768	PPA_euphoria	0.898		
2	Sens_hi stress	0.629	PPA_hi stress	0.759	Acc	0.747
	Sens_low stress	0.879	PPA_low stress	0.659		
	Sens_disappointment	0.690	PPA_disappointment	0.606		
	Sens_euphoria	0.768	PPA_euphoria	0.883		
3	Sens_hi stress	0.514	PPA_hi stress	0.783	Acc	0.734
	Sens_low stress	0.879	PPA_low stress	0.644		
	Sens_disappointment	0.733	PPA_disappointment	0.564		
	Sens_euphoria	0.775	PPA_euphoria	0.887		
4	Sens_hi stress	0.778	PPA_hi stress	0.778	Acc	0.766
	Sens_low stress	0.727	PPA_low stress	0.750		
	Sens_disappointment	0.793	PPA_disappointment	0.575		
	Sens_euphoria	0.768	PPA_euphoria	0.898		
5	Sens_hi stress	0.778	PPA_hi stress	0.875	Acc	0.804
	Sens_low stress	0.818	PPA_low stress	0.771		
	Sens_disappointment	0.828	PPA_disappointment	0.632		
	Sens_euphoria	0.800	PPA_euphoria	0.889		
6	Sens_hi stress	0.722	PPA_hi stress	0.813	Acc	0.762
	Sens_low stress	0.848	PPA_low stress	0.757		
	Sens_disappointment	0.759	PPA_disappointment	0.564		
	Sens_euphoria	0.743	PPA_euphoria	0.867		
7	Sens_hi stress	0.694	PPA_hi stress	0.833	Acc	0.766
	Sens_low stress	0.848	PPA_low stress	0.737		
	Sens_disappointment	0.862	PPA_disappointment	0.568		
	Sens_euphoria	0.725	PPA_euphoria	0.909		
8	Sens_hi stress	0.833	PPA_hi stress	0.811	Acc	0.810
	Sens_low stress	0.879	PPA_low stress	0.784		
	Sens_disappointment	0.759	PPA_disappointment	0.667		
	Sens_euphoria	0.786	PPA_euphoria	0.902		
9	Sens_hi stress	0.806	PPA_hi stress	0.744	Acc	0.744
	Sens_low stress	0.758	PPA_low stress	0.714		
	Sens_disappointment	0.655	PPA_disappointment	0.528		
	Sens_euphoria	0.743	PPA_euphoria	0.897		
10	Sens_hi stress	0.722	PPA_hi stress	0.813	Acc	0.768
	Sens_low stress	0.788	PPA_low stress	0.743		
	Sens_disappointment	0.655	PPA_disappointment	0.594		
	Sens_euphoria	0.829	PPA_euphoria	0.841		

by using the captured videos for reevaluation of the experts' decision. During the experimental procedure, the multisensorial balaclava is not used (only the sensors are attached in the subjects' face); thus, the experts can assess the subjects' emotional state according to their facial expression.

The raw signals (facial EMG, ECG, respiration, and EDA), which are obtained previously, are first segmented in windows of 10 s. Then, for each 10-s period, the feature-extraction module extracts from the signals the features described in Section II-B. The next step is to construct a vector containing the extracted features along with the experts' annotation (for the specific 10-s period). These vectors, for each subject and driving round (1676 vectors in total: high stress—358, low stress—330, disappointment—291, and euphoria—697), constitute our dataset which is used to train and test the classifiers. By using tenfold cross validation, the SVM classifier achieved an overall classification accuracy of 79.3%, whereas the ANFIS classifier achieved an overall classification accuracy of 76.7%. Tables II and III present the results for the SVM and ANFIS classifiers, respectively. Furthermore, in Tables IV and V, the confusion matrices for SVM and ANFIS are presented. Finally, the robustness of the classification is demonstrated in Table VI, where the tenfold cross-validation results for the two classifiers used are summarized, indicating low standard deviations.

IV. DISCUSSION

In this paper, we present a novel approach in emotion recognition. In addition, we describe a wearable system which can be used by car-racing drivers. Our system classifies basic human emotional states in near real time. The emotional states addressed are the following: high stress, low stress, euphoria, and disappointment.

According to our approach, the selected physiological signals are converted into extracted features. A dataset is created

TABLE IV
CONFUSION MATRIX FOR THE SVM CLASSIFIER

	High Stress	Low Stress	Disappointment	Euphoria
Classified as High Stress	268	17	22	18
Classified as Low Stress	46	276	20	25
Classified as Disappointment	24	15	221	90
Classified as Euphoria	20	22	28	564

TABLE V
CONFUSION MATRIX FOR THE ANFIS CLASSIFIER

	High Stress	Low Stress	Disappointment	Euphoria
Classified as High Stress	260	19	20	27
Classified as Low Stress	49	269	22	30
Classified as Disappointment	31	21	219	103
Classified as Euphoria	18	21	30	537

containing the extracted features along with the expert's annotation for each 10-s period. This time window is a significant factor, for the output of the intelligent emotion recognition module, since it determines how often it will provide updates about the emotional state of a user. The objective of a real time or near real-time emotion classifier is to first recognize as correctly as possible the emotional state of the user (high classification rate) and then to recognize it as soon as possible (high sensitivity). The former suggests a large window size to minimize variance in the features within a class. On the contrary, the latter suggests a small window size. The 10-s period window has been selected as the suitable compromise between these two arguments, based on the fact that there is a time delay between the instance that the subject experienced an emotion and the corresponding response changes in the selected biosignals [21].

The overall classification accuracy is high. Table VII presents the classification results of other biosignal-based emotion recognition methods reported in the literature. Picard *et al.* [1] reported higher classification accuracy in eight emotional classes; however, the evaluation was performed by using only one subject. It must be emphasized that since the other methodologies have been applied in different datasets, containing different types of biosignals and involving dissimilar emotional classes, a direct comparison between the obtained results is not feasible. The results obtained in this paper, although promising, are indicative. Due to the fact that emotions vary from person to person, the system must be trained by using a variety of subjects in real conditions and then tested for its performance. It should be noted that the emotional classes (high stress, low stress, euphoria, and disappointment) have been selected, keeping in mind that the experiments have been conducted in simulated race conditions. According to the psychologists evaluating the experiment, emotions do not always correlate with specific driving events, and subjects may experience different emotions during the same situation (driving event), depending on their personalities. Moreover, it is very likely that a subject driving in simulated conditions expresses disappointment instead of fear. This indicates that in real-life conditions, the emotional states might be altered, and thus, new classes might be added.

There is no perfect algorithm that is optimal under all conditions. Given specific application, sensor suite, and inference requirements to be achieved, there are generally a number of competing algorithms which are applicable to the processing of the data. In addition, the field of emotion recognition is not a trivial one but rather presents significant challenges to the associated researchers. Thus, SVM and ANFIS were utilized due to their well-known capabilities which are applicable to a variety of different pattern-recognition tasks [24]. In our approach, the use of SVM is advantageous since it improves the efficiency of the proposed system. On the other hand, ANFIS overall accuracy achieved was comparable with the SVM. The use of these two classifiers demonstrated the potential of our approach. However, only the application of the system in real conditions will provide a better insight into the underlying inference process and make the selection of the most appropriate classifier feasible.

Our system provides a useful tool for the mechanics of car-racing teams since they will be able to correlate the emotional state of the driver with specific adjustments in the car's performance. Moreover, the car's setting and development will not only be based in subjective questionnaires filled by the driver but also in the driver's emotional state which may interrelate with the car's performance. The adjustments on the car performance will have an impact on the driver's emotional state, and it may reduce accidents in car racings. On the other hand, emotions and psychological situation generally affect the driver's behavior and reactions. Thus, if some emotion is detected that in some way may affect the behavior of the user, then the observer will be able to provide him with additional pieces of advice and guidance, preventing some reaction of the user that would be fateful.

The system could also be utilized in several medical application fields. Clinical applications will be based on the ability to support clinical diagnosis related to all cases when the patient's capability to feel and express emotions is limited or totally absent. The main clinical activities could deal with the nervous system and its disorders such as Parkinson's disease, Huntington's disease, cortical lesion, and stroke. In those cases, doctors need to know the psychological condition of their patients. The goal is to evaluate the emotional state of the subject/patient. However, the use of specific drugs temporarily normalizes or even decreases the facial muscular activity. Using the proposed system, we will be able to follow the response of the patient to the specific drugs, adjusting and optimizing the dosages prescribed.

TABLE VI
SUMMARY OF THE TENFOLD CROSS-VALIDATION RESULTS FOR THE SVM AND ANFIS CLASSIFIERS

	SVM classifier						ANFIS Classifier					
	Sens		PPA		Accuracy		Sens		PPA		Accuracy	
class	average	std	average	std	average	std	average	std	average	std	average	std
high stress	0.748	0.077	0.829	0.053			0.725	0.095	0.799	0.038		
low stress	0.837	0.067	0.756	0.051	0.793	0.021	0.815	0.061	0.731	0.046	0.767	0.024
disappointment	0.756	0.056	0.636	0.065			0.753	0.070	0.587	0.039		
euphoria	0.809	0.029	0.891	0.032			0.771	0.030	0.887	0.019		

TABLE VII
PERFORMANCE OF THE BIOSIGNAL-BASED EMOTION RECOGNITION METHODS REPORTED IN THE LITERATURE

Author	Classification Method	Emotional classes	Data type	Classification accuracy (%)
Flidlund *et al.* 1983	Linear Discriminants	Happy, sad, anger, fear	4 facial EMGs	51.0
Haag *et al.* 2004	ANN	Arousal	EMG, EDA, skin temperature, BVP, ECG, Respiration	89.9
Haag *et al.* 2004	ANN	Valence	EMG, EDA, skin temperature, BVP, ECG, Respiration	96.0
Kim *et al.* 2004	SVM	Sadness, anger, stress, surprise	ECG, skin temperature, EDA	61.8
Picard *et al.* 2001	Fisher Projection	Neutral, anger, hatred, grief, platonic love, romantic love, joy, reverence	1 facial EMG, blood volume pulse, EDA, respiration effort	81.0
This work	**ANFIS-SVM**	**high stress, low stress, disappointment, euphoria**	**4 facial EMGs, ECG, respiration, EDA**	**76.7-79.3**

V. CONCLUSION

A novel methodology that automatically monitors and classifies the psychological condition of human subjects from a set of emotions, by applying pattern recognition techniques, is presented. The usual way to assess human emotion is by employing advanced image processing techniques in order to extract the facial characteristics. In our case, these techniques are not applicable since for safety reasons, the drivers are wearing a casque. Our methodology estimates the emotional state of human subjects by classifying features extracted from facial EMG, ECG, respiration, and EDA biosignals. The methodology has been transferred to a wearable system which is designed for car-racing drivers. The evaluation of the system in simulated race environment has shown high performance.

REFERENCES

[1] R. W. Picard, E. Vyzas, and J. Healey, "Toward machine emotional intelligence: Analysis of affective physiological state," *IEEE Trans. Pattern Anal. Mach. Intell.*, vol. 23, no. 10, pp. 1175–1191, Oct. 2001.

[2] J. Healey and R. Picard, "Digital processing of affective signals," in "Perceptual Computing Session," M.I.T. Medial Lab., Seattle, WA, Tech. Rep. No. 444, 1998.

[3] I. Essa and A. Pentland, "A vision system for observing and extracting facial action parameters," in *Proc. CVPR*, 1994, pp. 76–83.

[4] I. Essa and A. Gardner, "Prosody analysis for speaker affect determination," in *Proc. Workshop Perceptual User Interfaces*, 1997, pp. 45–46.

[5] L. C. DeSilva, T. Miyasato, and R. Nakatsu, "Facial emotion recognition using multi-modal information," in *Proc. IEEE Intell. Conf. Inf., Commun., Signal Process.*, 1997, pp. 397–401.

[6] J. T. Cacioppo and L. G. Tassinary, "Inferring physiological significance from physiological signals," *Amer. Psychol.*, vol. 45, no. 1, pp. 16–28, Jan. 1990.

[7] P. Ekman and W. Friesen, *Unmasking the Face*. Englewood Cliffs, NJ: Prentice-Hall, 1975.

[8] K. Anderson and P. W. McOwan, "A real-time automated system for the recognition of human facial expressions," *IEEE Trans. Syst., Man, Cybern. B, Cybern.*, vol. 36, no. 1, pp. 96–105, Feb. 2006.

[9] M. J. Black and Y. Yacoob, "Tracking and recognizing rigid and non-rigid facial motions using local parametric models of image motion," in *Proc. Int. Conf. Comput. Vis.*, 1995, pp. 374–381.

[10] M. Black and Y. Yaccob, "Recognizing facial expressions in image sequences using local parameterized models of image motion," *Int. J. Comput. Vis.*, vol. 25, no. 1, pp. 23–48, Oct. 1997.

[11] G. Donato, M. S. Barlet, J. C. Hager, P. Ekman, and T. J. Sejnowski, "Classifying facial actions," *IEEE Trans. Pattern Anal. Mach. Intell.*, vol. 21, no. 10, pp. 974–989, Oct. 1999.

[12] M. S. Bartlett, J. C. Hager, P. Ekman, and T. J. Sejnowski, "Measuring facial expressions by computer image analysis," *Psychophysiology*, vol. 36, no. 2, pp. 253–263, Mar. 1996.

[13] L. S. Chen, A. Huang, T. Miyasato, and R. Nakatsu, "Multimodal human emotion expression recognition," in *Proc. 3rd. Int. Conf. Face Gesture Recog.*, 1998, pp. 366–371.

[14] T. S. Huang, L. S. Chen, and H. Tao, "Bimodal emotion recognition by man and machine," in *Proc. ATR Workshop Virtual Commun. Environ.*, 1998, pp. 1–7.

[15] C. M. Jones and I. M. Jonnson, *Automatic Recognition of Affective Cues in the Speech of Car Drivers to Allow Appropriate Responses*, 2005.

[16] P. Ekman, R. W. Levenson, and W. V. Friesen, "Autonomic nervous system activity distinguishes among emotions," *Science*, vol. 221, no. 4616, pp. 1208–1210, Sep. 1983.

[17] W. M. Winton, L. Putnam, and R. Krauss, "Facial and autonomic manifestations of the dimensional structure of emotion," *J. Exp. Soc. Psychol.*, vol. 20, pp. 195–216, 1984.

[18] A. J. Flidlund and E. Z. Izard, "Electromyographic studies of facial expressions of emotions and patterns of emotions," in *Social Psychophysiology: A Sourcebook*. New York: Guilford Press, 1983, pp. 243–286.

[19] J. T. Cacioppo, J. T. Berntson, K. M. Larsen, K. Poehlman, and T. A. Ito, *The Psychophysiology of Emotion*, M. Lewis, A. Haviland, and C. M. Jones, Eds. New York: Guilford Press, 2000.

[20] J. Healey, "Wearable and Automotive Systems for Affect Recognition From Physiology," Ph.D. dissertation, MIT, Cambridge, MA, 2000.

[21] M. E. Dawson, A. M. Schell, and D. L. Filion, *Handbook of Psychophysiology*. New York: Cambridge Univ. Press, 2000.
[22] A. Haag, S. Gornzy, P. Schaich, and J. Williams, "Emotion recognition using bio-sensors: First steps towards an automatic system," in *Affective Dialogue Systems*. New York: Springer-Verlag, 2004, pp. 36–48.
[23] C. D. Katsis, N. Katersidis, G. Ganiatsas, and D. I. Fotiadis, "Aubade—A wearable EMG augmentation system for robust emotional understanding," in *Proc. ICICTH*, 2005, pp. 292–297.
[24] K. H. Kim, S. W. Bang, and S. R. Kim, "Emotion recognition system using short-term monitoring of physiological signals," *Med. Biol. Eng. Comput.*, vol. 42, no. 3, pp. 419–427, May 2004.
[25] L. James, *Road Rage and Aggressive Driving*. Amherst, NY: Prometheus Books, 2000.
[26] E. R. Kandel and J. H. Schwartz, *Principles of Neural Science*. New York: McGraw-Hill, 2000.
[27] F. J. McGuigan, *Cognitive Psychophysiology: Principles of Covert Behaviour*. Englewood Cliffs, NJ: Prentice-Hall, 1978.
[28] C. D. Katsis, N. E. Ntouvas, C. G. Bafas, and D. I. Fotiadis, "Assessment of muscle fatigue during driving using surface EMG," in *Proc. 2nd IASTED Int. Conf. Biomed. Eng.*, 2004, pp. 259–262.
[29] T. Takahashi, T. Murata, T. Hamada, M. Omori, H. Kosaka, M. Kikuchi, H. Yoshida, and Y. Wada, "Changes in EEG and autonomic nervous activity during meditation and their association with personality traits," *Int. J. Psychophysiol.*, vol. 55, no. 2, pp. 199–207, Feb. 2005.
[30] J. M. Gorman, J. D. Martinez, J. D. Coplan, J. Kent, and M. Kleber, "The effect of successful treatment on the emotional and physiological response to carbon dioxide inhalation in patients with panic disorder," *Biol. Psychiatry*, vol. 56, no. 11, pp. 862–867, Dec. 2004.
[31] M. Helander, "Applicability of drivers' electrodermal response to the design of the traffic environment," *J. Appl. Psychol.*, vol. 63, no. 4, pp. 481–488, Aug. 1978.
[32] W. D. Fenz and S. Epstein, "Gradients of physiological arousal in parachutists as a function of an approaching jump," *Psychosom. Med.*, vol. 29, no. 1, pp. 33–51, Jan./Feb. 1967.
[33] A. Norman, "The validity and reliability of polygraph decisions in real cases," *Polygraph*, vol. 19, pp. 169–181, 1990.
[34] P. Ekman, "Facial expression and emotion," *Amer. Psychol.*, vol. 48, pp. 384–392, 1993.
[35] P. J. Lang, M. M. Bradley, and B. N. Cuthbert, *International Affective Picture System (IAPS): Technical Manual and Affective Ratings*, 1988.
[36] J. A. Russell, "A circumplex model of affect," *J. Pers. Soc. Psychol.*, vol. 39, no. 6, pp. 1161–1178, Dec. 1980.
[37] V. N. Vapnik, *The Nature of Statistical Learning Theory*. New York: Springer-Verlag, 1995.
[38] C.-C. Chang and C.-J. Lin, *LIBSVM: A Library for Support Vector Machines, Software*, 2001. (last time accessed 22/11/06). [Online]. Available: http://www.csie.ntu.edu.tw/~cjlin/libsvm
[39] J. T. Jang, C. T. Sun, and E. Mizutani, *Neuro Fuzzy and Soft Computing*, ser. Matlab Curriculum Series. Englewood Cliffs, NJ: Prentice-Hall, 1997.
[40] M. Sugeno, *Industrial Applications of Fuzzy Control*. Amsterdam, The Netherlands: Elsevier, 1985.
[41] R. Kohavi, "A study of cross-validation and bootstrap for accuracy estimation and model selection," in *Proc. 14th IJCAI*, 1995, pp. 1137–1145.
[42] L. Breiman, J. H. Friedman, R. A. Olsen, and C. J. Stone, *Classification and Regression Trees*. Pacific Grove, CA: Wadsworth & Brooks, 1984.

Christos D. Katsis was born in Preveza, Greece, in 1972. He received the B.S. degree from the University of Ioannina, Ioannina, Greece, where he is currently working toward the Ph.D. degree in the Department of Medical Physics, Medical School.

He is also currently with the Unit of Medical Technology and Intelligent Information Systems, Department of Computer Science, University of Ioannina. His research interests include decision support systems in healthcare, electromyogram (EMG) analysis, pattern recognition, and automated diagnosis in EMG.

Nikolaos Katertsidis received the B.Eng. degree in electronic systems engineering from the University of Manchester Institute of Science and Technology, Manchester, U.K., and the M.Sc. degree in communications and signal processing from Imperial College, London, U.K.

Previously, he was with Huntchison 3G, U.K., as a Radio Planning Engineer, with Lehman Brothers, U.K., as a Network Systems Engineer, and with Hellenic Army (Signal Corps) as a Communications Engineer. Since 2004, he has been with the Unit of Medical Technology and Intelligent Information Systems, Department of Computer Science, University of Ioannina, Ioannina, Greece, working on R&D tasks.

George Ganiatsas was born in Youngstown, OH, in 1974. He received the B.Sc. degree with a double major in computer science and mathematics from Youngstown State University, Youngstown, in 1996.

He is currently an External Senior Software Engineer with the Unit of Medical Technology and Intelligent Information Systems, Department of Computer Science, University of Ioannina, Ioannina, Greece. He has managed many national and European projects as a Technical Supervisor.

Dimitrios I. Fotiadis (M'01–SM'07) was born in Ioannina, Greece, in 1961. He received the Diploma degree in chemical engineering from the National Technical University of Athens, Athens, Greece, and the Ph.D. degree in chemical engineering from the University of Minnesota, Minneapolis.

Since 1995, he has been with the Department of Computer Science, University of Ioannina, Ioannina, where he is currently an Associate Professor and the Director of the Unit of Medical Technology and Intelligent Information Systems. He is also currently with the Biomedical Research Institute—Foundation of Research and Technology Hellas, Ioannina. His research interests include biomedical technology, biomechanics, scientific computing, and intelligent information systems.